

## Mode Conversion and Local Heating below the Second Electron Cyclotron Harmonic

H. Sugai<sup>(a)</sup>

*Institute of Plasma Physics, Nagoya University, Nagoya 464, Japan*

(Received 26 October 1981)

If an extraordinary wave is normally incident on a large volume magnetoplasma, then below the second gyroharmonic, conversion into short-wavelength Bernstein waves is observed near the upper-hybrid layer. Significant conversion efficiency is attained in the optimum conditions. For high power incidence, considerable electron heating due to the converted wave is found to be localized in the mode-conversion region.

PACS numbers: 52.40.Db, 52.50.Gj

Recently much attention has been given to mode-conversion processes from an electromagnetic wave of the extraordinary mode to an electrostatic wave of the Bernstein mode. These processes play the crucial role in electron cyclotron heating of fusion plasmas,<sup>1</sup> as well as in laser-plasma interactions in self-generated magnetic fields.<sup>2</sup> Experiments<sup>3</sup> on transmission and emission of microwaves have revealed plasma column resonances<sup>4</sup> below the electron second gyroharmonic, which are attributed to radial standing waves of the Bernstein mode (wavelength  $\lambda_{\perp}$ ) excited by mode conversion. However, these measurements were performed outside a plasma column of small diameter  $d \approx \lambda_{\perp}$ , while Bernstein modes excited by electrostatic coupling (not by the conversion) have been detected inside plasmas.<sup>5</sup> In the present work, I have reported the first direct observations of mode-conversion processes inside an unusually large ( $d \gg \lambda_{\perp}$ ) plasma, together with the conversion efficiency measurement and the local electron heating due to the converted waves.

In the cold-plasma approximation, the refractive index  $n (= ck_{\perp}/\omega)$  of an extraordinary mode ( $X$  mode) is given by<sup>1</sup>

$$n^2 = - \frac{[\omega_p^2 - \omega(\omega + \omega_c)][\omega_p^2 - \omega(\omega - \omega_c)]}{\omega^2(\omega_p^2 + \omega_c^2 - \omega^2)}, \quad (1)$$

where  $\omega_p$  and  $\omega_c$  are the electron plasma and cyclotron frequencies, respectively. When the finite-Larmor-radius effect is taken into account, an electron Bernstein mode appears as shown in Fig. 1, where the wave frequency is assumed below the second gyroharmonic ( $\omega/\omega_c = 1.9$ ). For constant magnetic field,  $\omega_p^2/\omega_c^2$  is proportional to the plasma density. Thus, the slow  $X$  mode propagating to the lower-density side converts into the Bernstein mode at the cold-plasma upper-hybrid-resonance layer ( $\omega_p^2 = \omega^2 - \omega_c^2$ ). On the other hand, the fast  $X$  mode inci-

dent from outside the plasma tunnels through the evanescent region between the cutoff [ $\omega_p^2 = \omega(\omega - \omega_c)$ ] and the resonance layers, and converts into both the Bernstein and the slow  $X$  mode.

The experiment is performed in a pulsed discharge plasma produced in argon at  $3 \times 10^{-4}$  Torr, with an oxide-coated cathode of 60 cm diam. The plasma characteristics are  $\kappa T_e \approx 1.5$  eV,  $\kappa T_i \approx 0.2$  eV, density  $N = 10^9 - 10^{12}$  cm<sup>-3</sup>, diameter  $d \approx 70$  cm, length  $\approx 3$  m, and uniform axial magnetic field  $B_0 < 500$  G. The radial density gradient is variable in the range  $3 < N/(\partial N/\partial r) < 40$  cm, by a gradient control grid. Microwaves of frequencies 0.75–3.0 GHz are launched radially from open-waveguide antennas located outside the plasma column. Spatial profiles of microwave field in the plasma are detected with a short (3-mm) coax-fed wire antenna movable radially. The detected signal is amplified and applied to an interferometer circuit whose output is proportional to the wave power  $p(r) \cos(k_{\perp} r)$ .

Mode conversions are found below the second

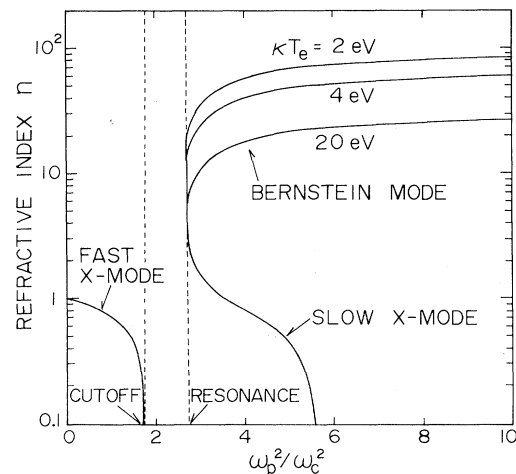


FIG. 1. Refractive index  $n$  vs  $\omega_p^2/\omega_c^2$  for  $\omega/\omega_c = 1.9$ .

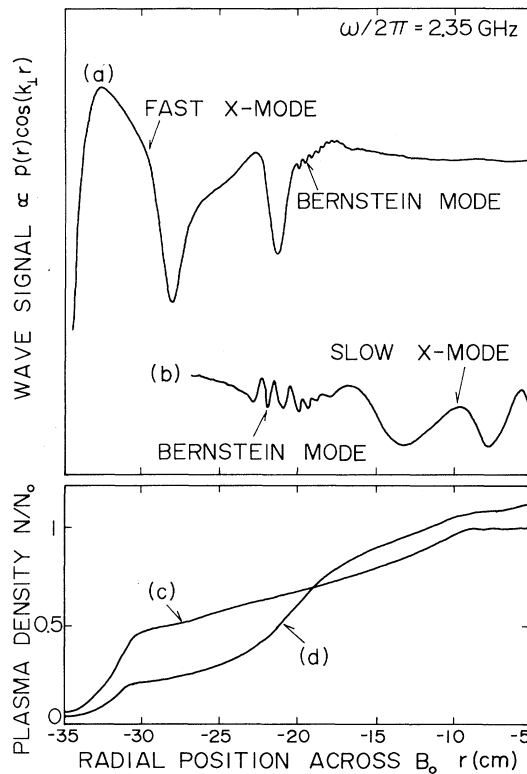


FIG. 2. Interferometer traces for the microwave incident (a) from outside the plasma at  $\omega/\omega_c = 1.95$ , and (b) from within the plasma at  $\omega/\omega_c = 1.97$ , together with (c) gentle and (d) steep radial profiles of the plasma density.

gyroharmonic ( $\omega/\omega_c \lesssim 2$ ). Figure 2 shows the conversion from the fast X mode to the Bernstein mode, which is observable in such a steep density profile as shown in Fig. 2(d). The fast X mode is launched from  $r = -38$  cm, is reflected at the cutoff layer ( $r \approx -21$  cm), and forms the standing wave which gives rise to visible distortion in the interferometer pattern. The apparent damping of the X mode is attributed to the geometrical divergence of waves from the launcher. Beyond the upper-hybrid layer ( $r \approx -20$  cm), the short-wavelength ( $\sim 5$  mm) Bernstein mode is observed with the long-wavelength component of the transmitted slow X mode. Figure 2(b) shows the conversion from a slow X mode to a Bernstein mode in the gentle density profile shown in Fig. 2(c). In this case, the X mode is incident from within the plasma, from a shielded magnetic loop antenna (1.5 cm in diameter) at  $r = 2$  cm. At the hybrid layer ( $r = -24$  cm), the X mode converts into the Bernstein mode which propagates back to the higher density side.

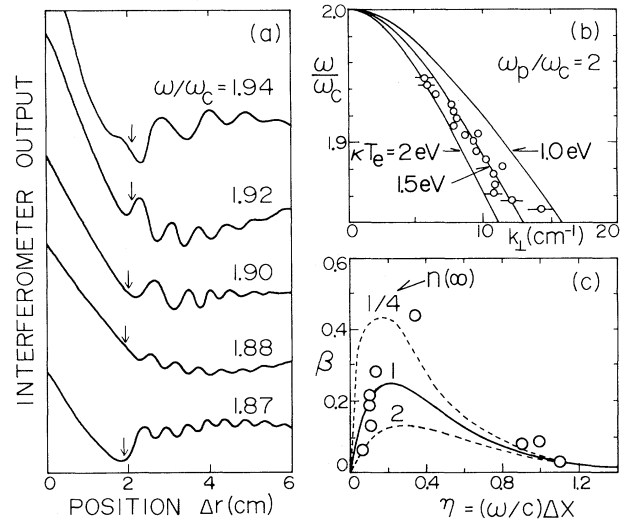


FIG. 3. (a) Interferometer traces for several values of  $\omega/\omega_c$ . Arrows indicate the hybrid-resonance points.  $\omega_c/2\pi = 411$  MHz. (b) Experimental points and theoretical curves of Bernstein-wave dispersion relation.  $\omega_c/2\pi = 347$  MHz. (c) Efficiency  $\beta$  of mode conversion into a Bernstein mode of an extraordinary wave incident from outside the plasma.

To identify the excited wave of short wavelength, I measured the perpendicular wave number  $k_\perp$  by interferometry and in Fig. 3(a) typical radial interferometer patterns are shown for the fast X mode incident from outside the plasma. The wave exhibits a cutoff ( $\lambda_\perp \rightarrow \infty$ ) for  $\omega \approx 2\omega_c$ , and  $\lambda_\perp$  decreases with  $\omega/\omega_c$ . The wavelength at constant  $\omega/\omega_c$  decreases with increasing  $\Delta r$  (increasing the density). In Fig. 3(b), I have plotted the wave dispersion measured at a fixed radial position and find excellent agreement with the theoretical curve for  $\kappa T_e = 1.5$  eV (consistent with the Langmuir probe measurement). Theoretical curves are demonstrated for parallel wave number  $k_\parallel (= 2\pi/\lambda_\parallel) = 0$ , since the finite  $k_\parallel (< 1 \text{ cm}^{-1})$  does not modify appreciably the dispersion for  $k_\perp > 5 \text{ cm}^{-1}$ . Electron-neutral and electron-ion collisions are so rare ( $\nu/\omega \sim 10^{-5}$ ) that the wave damping is governed by cyclotron damping. In Fig. 3(a), the damping rate is found to become large as  $\omega/\omega_c \rightarrow 2$ . Agreement with the theoretical damping rate is obtained for  $\lambda_\parallel \sim 10$  cm, which is comparable to the parallel dimension of the launcher. From these measurements I conclude that the excited wave is indeed the Bernstein mode.

The conversion efficiency  $\beta$  from the fast X mode to the Bernstein mode can be estimated by

$\beta = 1 - R - T$ , if the power densities of reflection  $R$  and transmission  $T$  are known. Comparing Fig. 2(a) with 2(b), we note that the conversion efficiency  $\alpha$  from the slow  $X$  mode to the Bernstein mode is much greater than  $\beta$ . Mode-conversion theories<sup>6,7</sup> predict  $\alpha = 1 - \exp(-\pi\eta)$ , where  $\eta = (\omega/c)\Delta x$  and  $\Delta x$  is the distance between the cutoff and the resonance layers. So, in the gentle ( $\eta \approx 4.5$ ) profile shown in Fig. 2(c), almost complete conversion is expected. Now I can calibrate the detector sensitivity for the Bernstein mode relative to the  $X$  mode, assuming 100% conversion in Fig. 2(b). This calibration enables us to determine  $\beta$  with the aid of a measurement of the standing-wave ratio,  $(1-R)/(1+R)$ , in the underdense region. In this way, I have measured the efficiency, controlling the density gradient at the hybrid layer by means of the gradient control grid. The results are plotted in Fig. 3(c), as a function of  $\eta$ , i.e., the width of the tunneling region measured in free-space wavelengths.

The efficiency  $\beta$  has been obtained analytically<sup>6,8</sup> only for the density profile specified by the simple model index  $n^2(s) = a + \eta/s$ , where normalized position is  $s = \omega x/c$ , and the constant is  $a = 1$  for  $s < 0$ , and  $a = n^2(\infty)$  for  $s > 0$ . According to Eq. (1) for  $\omega/\omega_c \approx 2$ , for example, the constants  $n(\infty) = \frac{1}{2}$ , 1, and 2 give the densities ( $s \rightarrow \infty$ )  $\omega_p^2/\omega^2 = 1.45$ , 1, and 0.8, respectively. The special case of  $n(\infty) = 1$  corresponds to Budden's solution,<sup>6</sup>  $\beta = \exp(-\pi\eta) - \exp(-2\pi\eta)$ , which is indicated by the solid line in Fig. 3(c). In this experiment, the density in the overdense region ( $s > 0$ ) often exceeds  $\omega_p^2/\omega^2 = 1.45$ , and the overall density does not realize the theoretical models.<sup>6-9</sup> Qualitatively, however, the measurements have verified the existence of the best  $\eta$ , i.e., the best gradient scale length.

A 0.92-GHz, 10-kW, pulsed microwave source is used in order to study nonlinear effects<sup>10,11</sup> on the mode-conversion process. Figure 4(a) shows the interferometer traces sampled during the microwave burst of 2 kW and 1.3  $\mu$ s. Figure 4(b) displays the radial profiles of the ion saturation current collected by a Langmuir probe. The sampling time is delayed by 1  $\mu$ s after the turnoff of the microwave burst, in order to prevent Langmuir probe measurements from errors due to rf fields. As seen in Fig. 4(b), the ion current anomalously increases in the mode-conversion region ( $6 < \Delta r < 12$  cm). Figure 4(c) shows the electron temperature measured at the peak position ( $\Delta r \approx 9$  cm) by the probe. The tempera-

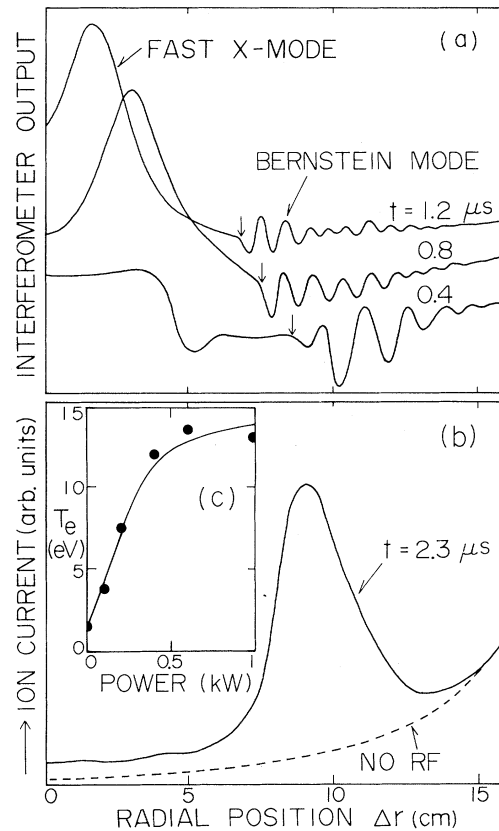


FIG. 4. (a) Wave signals sampled at different times  $t$  after the turnon of the microwave burst.  $\omega/\omega_c = 1.94$ . (b) Ion saturation current before (dashed line) and after (solid line) the microwave application. (c) Electron temperature vs incident microwave power.

ture increases with the incident power, but saturates around the ionization energy level (15.7 eV for argon), and then the plasma density increases as a result of ionization by heated electrons. Since the ion saturation current is proportional to  $NT_e$ , the density at  $\Delta r \approx 9$  cm is estimated to be tripled. Also, the wave measurements [Fig. 4(a)] support the density increase; the hybrid-resonance point indicated by arrows shifts toward the left and the wavelengths of the Bernstein mode become shorter with  $t$ .

A possibility of ionization by intense microwave fields is excluded because the pulse width is very short, and partly because although the microwave is more intense near the launcher ( $\Delta r < 5$  cm) there is less density change. For the incident power and the plasma parameters used, nonlinear ponderomotive-force effects of Bernstein waves are negligible<sup>10</sup> and dominated by the heating effect. The absence of the thresh-

old for the temperature rise suggests heating due to the cyclotron damping rather than parametric instabilities<sup>11</sup> of the converted Bernstein wave.

Fundamental processes observed in the present experiment are connected directly with pre-ionization by microwaves for the tokamak start-up.<sup>12</sup> Localized electron heating by slow as well as fast  $X$  modes is of interest for controlling the current and  $Q$  profiles of tokamak plasmas. Also, the mode-conversion process may predominantly contribute to the hot-electron ring formation at the second gyroharmonic region in bumpy tori.<sup>13</sup>

It is a pleasure to thank Dr. H. Ikegami, Dr. M. Fujiwara, Dr. M. Tanaka, and Dr. R. Sugihara for their interest and encouragement. The able assistance by Mr. S. Kishimoto and Mr. Y. Koji is greatly appreciated.

<sup>(a)</sup>Also at Department of Electrical Engineering, Nagoya University, Nagoya 464, Japan.

<sup>1</sup>T. H. Stix, Phys. Rev. Lett. **15**, 878 (1965); T. Mae-kawa, S. Tanaka, Y. Terumichi, and Y. Hamada, Phys.

Rev. Lett. **40**, 1379 (1978).

<sup>2</sup>C. Grebogi, C. S. Liu, and V. K. Tripathi, Phys. Rev. Lett. **39**, 338 (1977); W. Woo, K. Estabrook, and J. S. DeGroot, Phys. Rev. Lett. **40**, 1094 (1978).

<sup>3</sup>H. Dreicer, in *Plasma Waves in Space and in the Laboratory*, edited by J. O. Thomas and B. J. Landmark (University Press, Edinburgh, 1967), p. 157; B. B. O'Brien and H. H. Kuehl, Phys. Fluids **14**, 1187 (1971).

<sup>4</sup>S. J. Buchsbaum and A. Hasegawa, Phys. Rev. Lett. **12**, 685 (1964).

<sup>5</sup>F. Leuterer, Plasma Phys. **14**, 499 (1972), and references therein.

<sup>6</sup>K. G. Budden, *Radio Waves in the Ionosphere* (Cambridge Univ. Press, London, 1961), p. 476.

<sup>7</sup>Merit Shoucri and H. H. Kuehl, Phys. Fluids **24**, 1395 (1981).

<sup>8</sup>H. H. Kuehl, Phys. Rev. **154**, 124 (1967).

<sup>9</sup>R. Sugihara, J. Phys. Soc. Jpn. **21**, 786 (1966); R. B. White and F. F. Chen, Plasma Phys. **16**, 565 (1974).

<sup>10</sup>Merit Shoucri and H. H. Kuehl, Phys. Fluids **23**, 2461 (1980).

<sup>11</sup>A. T. Lin and Chih-Chien Lin, Phys. Rev. Lett. **47**, 98 (1981).

<sup>12</sup>R. M. Gilgenbach *et al.*, Nucl. Fusion **21**, 319 (1981).

<sup>13</sup>For example, Proceedings of Workshop on EBT Ring Physics, Oak Ridge, Tennessee, December 1979, edited by N. A. Uckan (unpublished).

## Toroidal Plasma Current Sustainment by Lower Hybrid Waves in the WT-2 Tokamak

M. Nakamura, T. Cho, S. Kubo, T. Shimosuma, H. Kawai, K. Yamazaki, T. Maekawa, Y. Terumichi, Y. Hamada,<sup>(a)</sup> and S. Tanaka

*Department of Physics, Faculty of Science, Kyoto University, Kyoto 606, Japan*

(Received 21 September 1981)

By injecting rf power  $P_{rf}$  near the lower hybrid frequency into an Ohmically heated plasma near the end of tokamak discharge in the WT-2, an rf-driven current-sustained plasma is produced and continues to exist during the rf injection period, the toroidal current ( $I_p \sim 10$  kA) being generated by the lower hybrid wave only without the Ohmic power. The efficiency of rf-driven current generation is high and attains  $I_p/P_{rf} \approx 0.9$  kA/kW at the plasma density  $n_e \approx 1.4 \times 10^{12}$  cm<sup>-3</sup>, with somewhat lower efficiency at higher density.

PACS numbers: 52.50.Gj, 52.55.Gb

Generating and sustaining a continuous toroidal current comprise one of the most important problems to be settled in order to realize steady-state operation of a tokamak reactor.<sup>1-4</sup> It has been predicted theoretically that a fast electron beam carrying the continuous current is produced by the quasilinear Landau damping of lower hybrid waves (LHW).<sup>1,2</sup> Recently, experiments on current drive by LHW were carried out in tokamaks<sup>5-7</sup> and a stellerator.<sup>8</sup> When the LHW-driven current  $I_{rf}$  was produced

in Ohmically heated plasmas, the plasma current  $I_p$ , composed of  $I_{rf}$  and the Ohmic current, increased slightly, while the loop voltage  $V_L$  decreased, since the time constant of the plasma current is too long to change  $I_p$  during the rf pulse. In this Letter, we report the first experiment in the WT-2 tokamak, for which the toroidal plasma is sustained by the LHW-driven current  $I_{rf}$  only. No Ohmic current was present.

The WT-2 tokamak<sup>6</sup> has an aluminum shell,